

Conformational and Dynamic Behavior of Polymer and Polyelectrolyte Chains in Dilute Solutions

Karel Procházka

Contents

1 Neutral Chains	2
2 Comments on the Differences Between Dilute and Concentrated Solutions	10
3 Polyelectrolyte Chains	11
4 Comments on Computer Studies of Polymer Conformations and Dynamics	17
5 The Persistence Length	19
References	22

Abstract This introductory chapter provides a brief (textbook-like) survey of important facts concerning the conformational and dynamic behavior of polymer chains in dilute solutions. The effect of polymer–solvent interactions on the behavior of polymer solutions is reviewed. The physical meanings of the terms good, θ -, and poor thermodynamic quality of the solvent are discussed in detail. Basic assumptions of the Kuhn model, which describes the conformational behavior of ideal flexible chains, are outlined first. Then, the correction terms due to finite bond angles and excluded volume of structural units are introduced, and their role is discussed. Special attention is paid to the conformational behavior of polyelectrolytes. The “pearl necklace” model, which predicts the cascade of conformational transitions of “quenched” polymer chains (i.e., of those with fixed position of charges on the chain) in solvents with deteriorating solvent quality, is described and discussed in detail. The incomplete (up-to-date) knowledge of the behavior of “annealed” (i.e., weak) polyelectrolytes and some characteristics of semiflexible chains are addressed at the end of the chapter.

Keywords Ideal polymer chain • Realistic polymer chain • Chain conformations • Solvent quality • Quenched polyelectrolyte • Annealed polyelectrolyte • Pearl necklace model • Persistence length

K. Procházka (✉)

Department of Physical and Macromolecular Chemistry, Faculty of Science,
Charles University in Prague, Hlavova 2030, 128 40 Prague 2, Czech Republic
e-mail: karel.prochazka@natur.cuni.cz

Before the reader (presumably a scientist engaged in fluorescence studies) starts to read this chapter, he should know the content and purpose of this introductory part to decide whether he needs to refresh his memory about fundamental facts related to the behavior of polymer chains or if he can skip this part. This short (textbook-like) chapter is not aimed at providing an exhausting survey and explanation of the conformational and dynamic behavior of dilute solutions of polymers, copolymers, and polyelectrolytes of various chain architectures. There exist numerous chapters in excellent textbooks explaining the fundamentals of the physical chemistry of polymer solutions [1–5] and very good reviews on this topic [6, 7]. This chapter has a different purpose. Here, we would like to emphasize differences in the behavior of low- and high-molar-mass compounds caused by (i) asymmetry in the sizes of the polymer species with respect to the other components of the mixture, (ii) connectivity of the polymer chains, and (iii) their flexibility. We would like to remind a researcher studying low-molar-mass compounds by fluorescence techniques about what he should be aware of and prepared for when entering the polymer field. We will focus particularly on the aspects of the conformational and dynamic behavior that are important for understanding the results of fluorescence studies on aqueous polyelectrolyte systems. However, first we will outline the basic features of the general behavior of flexible chains in simple solvents.

1 Neutral Chains

The behavior of real polymer chains (homopolymers and copolymers, also including polyelectrolytes) in dilute solutions is a result of an intricate interplay of a number of cooperating and competing forces. The dissolution process reflects both enthalpy and entropy changes in the whole system, i.e., not only those directly connected with polymer chains but also various solvent effects, e.g., rearrangement of the solvent molecules in the solvation shell and counterion effects in polyelectrolyte solutions. Because the most important differences between the properties of high- and low-molar-mass compounds follow from the unique properties of long chains, classical theories of neutral polymer solutions ignore the structure of the solvent and specific solvation effects, as well as tiny details in the chemical composition of the polymer chains, etc. They treat polymer solutions at a simple mean-field level, representing the polymer chain as a sequence of interconnected (relatively short) linear parts (segments). Depending on the level of accuracy of the physical description, the segments represent one or more repeating units and are either freely joined (without any angular limitations) or the arrangement of two or more successive segments is constrained (bond angles, restricted rotation around single bonds, etc.). Furthermore, the simplest models assume that the segments are short lines without excluded volumes and can intersect, while more advanced models employ self-avoiding segments. In polymer thermodynamics, the segment–solvent interactions, w_{PS} , are usually compared with segment–segment, w_{PP} , and solvent–solvent interactions, w_{SS} , which simplifies the description because the

thermodynamic quality of the solvent can be characterized by a single parameter. The commonly used Flory–Huggins parameter [8, 9] (proportional to T^{-1}), $\chi_{FH} = a/T = (z-2)\Delta w/(kT)$, where z is the average number nearest neighbors and k is the Boltzmann constant, is based on the difference between the cross-interaction and the arithmetic average of homo-interactions, $\Delta w = w_{PS} - 1/2(w_{PP} + w_{SS})$. It serves as a basis for classification and sorting solvents into two categories: thermodynamically good and bad (poor) solvents. Solvents of the first class dissolve high-molar-mass polymers because the segment–solvent interactions are “reasonably good.” The latter category comprises poor or alternatively called thermodynamically bad solvents, which, from the practical point of view, are non-solvents (precipitants). The solvents in a narrow region in between good and bad solvents are often called marginal solvents. The critical marginal solvent in between the two categories of solvents is called the “ θ -solvent.” From a practical point of view, it is necessary to keep in mind that one particular solvent can be good for some polymers and bad for other polymers (depending on the polarity, etc.).

Before we start discussing the physical meaning of the “ θ -solvent” (and its χ_{FH} value), we would like to briefly mention “favorable” and “unfavorable” interactions. In nonpolar systems of low-molar-mass organic molecules A and B, the cross-term, w_{AB} , can usually be approximated by the geometric average of the w_{AA} and w_{BB} interactions as $w_{AB} = \sqrt{(w_{AA}w_{BB})}$. This means (see any textbook on the physical chemistry of simple liquids or polymers) [10–13] that Δw is positive and the mixing of small nonpolar molecules (without specific interactions) is always endothermic. In other words, the mixing of two nonpolar liquids is an unfavorable process from the point of view of the enthalpy. However, it is also true that an overwhelming number of nonpolar molecules mix spontaneously because their intermixing is accompanied by a considerable increase in entropy. The entropy of mixing of polymer chains with a low-molar-mass solvent is significantly lower than that accompanying the mixing of small mobile molecules. This general feature of polymer solutions can be easily understood when we compare the motion of n_M small monomer molecules dissolved in a solvent before and after polymerization. Assume that this reaction leads to n_P flexible chains, each containing on average N monomers ($n_M = n_P N$). In the first case, i.e., before polymerization, each monomer can move independently in the whole volume and acquires high translational entropy, while, in the latter case, N connected monomer units always have to be close to each other and have to move together, which reduces the entropy of the system considerably (especially if N is high).

The popular and widely used F–H interaction parameter was originally introduced in a successful theory developed independently by Flory [14] and Huggins [8, 15] in the early 1940s to describe the properties of concentrated polymer solutions. Their simple mean-field theory is based on a lattice (Bragg–Williams) model of regular solutions [16] and derives the following expression for the Gibbs energy of mixing a polymer with a solvent:

$$\Delta G = nRT(x_1 \ln \varphi_1 + x_2 \ln \varphi_2 + x_1 \varphi_2 \chi) \quad (1)$$

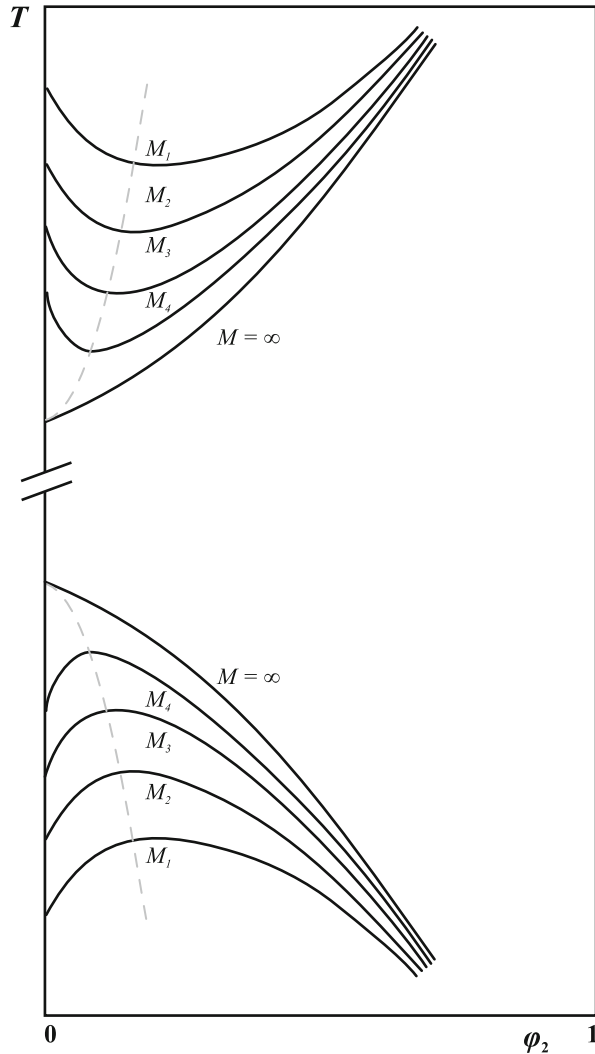
where n_i are the numbers of moles ($n = \sum n_i$); $x_i = n_i / \sum n_i$, the molar fractions; N_i are the degrees of polymerization (number of structural units in the chain: (1) solvent, $N_1 = 1$; (2) polymer, $N_2 \gg 1$); and $\varphi_i = N_i n_i / \sum N_i n_i$ are the volume fractions of the components. It is obvious that the entropy, i.e., the first two terms in Eq. (1), promotes the dissolution and the enthalpy (the last term) hinders it, but if χ_{FH} is not very positive, the Gibbs function of mixing can be negative and the polymer will dissolve in the solvent. As both the volume fractions, which are present in the two first terms, and the product $x_1 \varphi_2 \chi$ appearing in the third term, depend on the degree of polymerization, N_2 , increasing chain length hinders the dissolution and short chains dissolve in moderately poor solvents while long ones do not dissolve. Focusing on the behavior of infinitely long polymer chains, the theory yields the following value of the interaction parameter for the ϑ -solvent: $(\chi_{\text{FH}})_{\vartheta} = 1/2$. This value divides the solvents into the two categories described above. The F–H interaction parameters of good solvents theoretically range from 0 to $1/2$. Focusing on nonpolar systems (where the cross-term interaction obeys the geometric average rule), the best solvents (called “athermal” solvents) are those with $\chi_{\text{FH}} = 0$, but actual good solvents often have $\chi_{\text{FH}} \leq 0$ as a result of specific interactions (sometimes simply because of the high polarity of the components). Poor (bad) solvents are characterized by FH parameters $\chi_{\text{FH}} > 1/2$. The values of the F–H parameter depend on the temperature; the temperature, at which $\chi_{\text{FH}} = a/T = 1/2$, is often called the ϑ -temperature, ϑ (or ϑ -state). The simple F–H theory predicts that the solvent quality for a given polymer will improve with temperature. Above ϑ , chains of any length dissolve, i.e., also the infinitely long ones. At the ϑ -temperature, chains of infinite length start to separate into two liquid phases: a concentrated phase (i.e., the swollen polymer) and a dilute phase (in this case, the pure solvent). The chains of finite lengths start to separate into two phases at lower critical temperatures T_c , depending on the number of segments N_2 :

$$a/T_c = 1/2 + 1/\sqrt{N_2} + 1/(2N_2) \quad (2)$$

and below T_c , both coexisting phases (i.e., also the dilute one) contain finite concentrations of the polymer. The coexistence curves are schematically shown in the lower part of Fig. 1. Because ϑ is the highest critical temperature for a series of coexistence curves for chains differing in length, it is called the upper critical solution temperature (UCST), and the region of critical temperatures for chains of different length is called the UCST region.

The ϑ -temperature has an analogous meaning for polymer–solvent mixtures to the Boyle temperature for gasses: At this temperature, moderately unfavorable interactions between polymer segments and solvent molecules compensate the geometric excluded volume of the segments. The overall excluded volume (which reduces the volume available for the motion of the molecules) [17] drops to zero, and small as well as large molecules move as if the entire volume of the

Fig. 1 The coexistence curves. *Upper part:* the LCST region. *Bottom part:* the UCST region. The curves for infinitely long chains ($M = \infty$) separate the homogeneous (one-phase) region from the heterogeneous (two-phase) region



system were available. Hence, the conformations of the polymer chain at the ϑ -temperature are not affected by the excluded volume of the segments, and real self-avoiding chains behave as intersecting random walks.

At the end of this part, we would like to emphasize two important facts: First, because the F–H theory is a theory of regular polymer solutions and the cross-interaction term can be expressed as a geometric average of homo-interactions, the Gibbs function of mixing can be decomposed into parts corresponding to the pure components and to the entropy of mixing. Consequently, it is possible to predict the properties of polymer solutions at a semiquantitative level on the basis of the

properties of the pure components alone (see the appropriate chapters on the solubility parameters in any polymer textbook) [1, 16, 18].

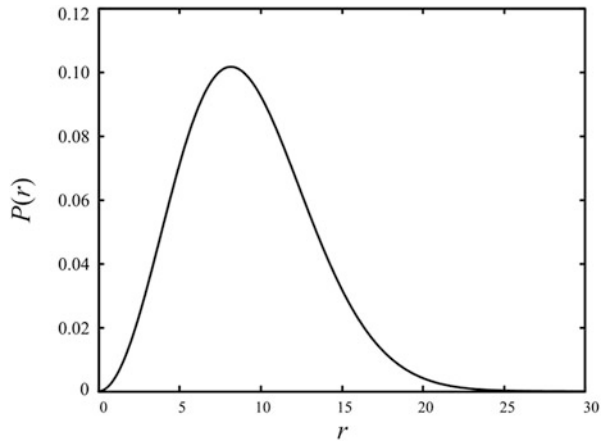
Second, we have seen that the F–H theory predicts an improvement in the solvent quality with temperature. However, at fairly high temperatures above the normal boiling point of the pure solvent (ca. $0.7\text{--}0.8 T_{\text{crit}}$, where T_{crit} is the critical temperature of the pure solvent), i.e., at elevated pressures, the solvent quality starts to deteriorate with increasing temperature, and the polymer solution phase separates upon heating. The worsening of solvent quality for high-molar-mass polymers at high temperatures is a general feature of polymer solutions, reflecting the fact that the thermal expansion of the solvent is significantly greater than that of the polymer. The solvent expands at high temperatures, and the solvent molecules have a quite large free volume for their motion; they move rapidly and acquire high translational entropy. Polymer dissolution requires proper solvation of the segments, which means that part of mobile solvent molecules has to “condense” on the chain. The solvating molecules lose their translational entropy, and since entropy plays an important role at high temperatures, the dissolution of the polymer chains is no longer favorable, and the solution separates into two phases. The coexistence curves are the mirror image of those in the UCST region (see the curves in the upper part of Fig. 1), and the critical temperature for the separation of infinitely long chains, which in this case is the lowest one, is called (somewhat paradoxically) the lower critical solution temperature (LCST). The F–H mean-field theory does not predict LCST and is applicable only in the region of UCST. In some aqueous solutions of neutral water-soluble polymers, LCST behavior is observed at relatively low temperatures because it is caused by specific effects reflecting changes in the water structure in the solvation layer, the formation of hydrogen bonds, etc. (e.g., phase separation occurs below $40\text{ }^\circ\text{C}$ in an aqueous solution of polyoxypropylene) [19, 20].

The simplest model for predicting the conformational characteristics of isolated flexible polymer chains was developed by Kuhn and Gr \ddot{u} n [21] and independently by James and Guth [22]. The chain is approximated by a sequence of segments of the same length l that are interconnected without any geometrical constraints, do not occupy geometrical volume, and do not interact over large distances. The corresponding interpenetrating chain is called an ideal chain. Mathematical treatment yields the distribution function of probability density that the ends of a chain composed of a large number N of segments are separated by distance r in the form (Fig. 2):

$$P(r) = 4\pi \left(\frac{3}{2\pi Nl^2} \right)^{\frac{3}{2}} \exp\left(\frac{-3r^2}{2Nl^2} \right) r^2 \quad (3)$$

Note that $P(r)$ is the angularly averaged function and does not depend on the direction of the end-to-end vector. In a narrow region of temperatures close to the θ -temperature, real chains behave as interpenetrating ones, and the model provides a qualitatively correct picture of the conformational behavior of flexible chains.

Fig. 2 The distribution function of probability density $P(r)$ that the ends of an ideal chain are separated by distance r



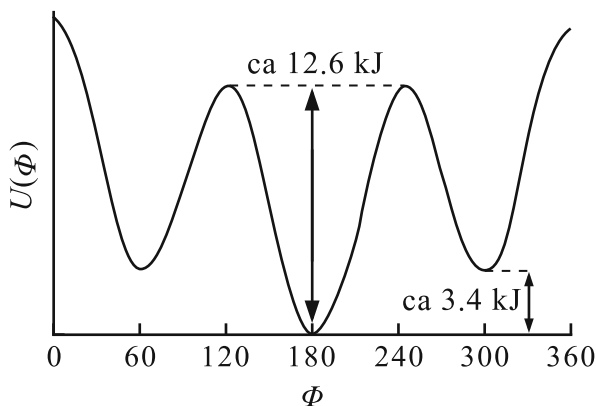
It predicts that (i) the chain adopts a random coil conformation, (ii) it responds to deformation as an entropic spring, and (iii) both the mean-square average end-to-end distance $\sqrt{\langle r^2 \rangle}$ and the radius of gyration R_G of the chain scale with $N^{1/2}$. Scaling exponent $1/2$ means that an ideal 3D polymer chain behaves as a nontrivial fractal object with fractal dimension 2, and its self-similar subunits exhibit the same conformational and scaling behavior as the whole chain. (iv) The conformational behavior of the chains is controlled by the entropy, and the characteristics of the coil depend on the total number of segments N , e.g., the average segment density in the coil domain is proportional to $N^{-1/2}$, which means that longer chains are relatively more expanded (with respect to the unit contour length) and form less dense coils than the shorter ones and (vi) the density profile decreases with the distance from the center of gravity according to the Gaussian function. The Gaussian density profile gave rise to the commonly used name “Gaussian chain.” The Monte Carlo and molecular dynamics simulations show that the chain shape fluctuates greatly and that the average ensemble shape is aspherical (the spherical symmetry of the chain characteristics predicted by the simple Kuhn model is derived from the a priori symmetry assumptions used in this theory) and corresponds to an elongated ellipsoid with relative lengths of the axes 1:1.6:3.5 [23].

Various corrections reflecting fixed valence bond angles, hindered rotation around single bonds, and the excluded volume of segments were developed later and are described in detail in textbooks [12, 24]. The scaling behavior of self-avoiding flexible chains was studied by de Gennes [25]. He proposed scaling of $\sqrt{\langle r^2 \rangle}$ and R_G with $r^{0.6}$. Perturbation theories and detailed computer simulations give a value of the scaling exponent of 0.588 and indicate that the average shape of the self-avoiding chain is also reminiscent of an elongated ellipsoid, similar to that representing the interpenetrating coil [26]. The conformational characteristics of real chains with possible rotation around single C–C bonds can be reasonably interpreted using the conclusions drawn from a simple analytical formula (3) without correction terms if we assume that one Kuhn segment represents a short

part of the chain. In this case, rotation around several single bonds ensures that the first and last bonds that connect such an internally flexible segment to the rest of the chain are oriented quite randomly without almost any limitations. The rescaling, i.e., evaluation of the number of Kuhn segments, N_K , and their effective length, l_K , can be based on the contour length, L_C , and the root-mean-square end-to-end distance, $\sqrt{\langle r^2 \rangle}$, because it has to hold that $L_C = Nl = N_K l_K$ and $\sqrt{\langle r^2 \rangle} = N^{1/2}l = N_K^{1/2}l_K$. If the experimental values l_K and the radius of gyration $R_G = (1/\sqrt{6})\sqrt{\langle r^2 \rangle}$ for real chains in ϑ -solvents are used [18], then the angular restrictions and hindered rotation are reasonably accounted for.

Another simple, albeit quite popular, model of flexible linear polymer chains is the rotational isomeric state model (RIS) amply treated by Flory [12, 27]. This model was in fact developed by three independent groups: Volkenstein et al. [28], Lifson [29], and Nagai [30]. Analyzing the hindered internal rotation in butane and in longer alkane chains $(-\text{CH}_2-)_n$, the authors of this model realized that the “cis” conformation of four successive bonds (or $-\text{CH}_2-$ groups) in the polyethylene chain is very improbable because it is an unstable conformation (characterized by an energy maximum on the energy vs. dihedral angle diagram—see Fig. 3) and its energy is very high (it is ca. 15 kJ/mol larger than that of the stable “trans” conformation characterized by a total energy minimum). Two other low-energy conformations are “+ gauche” and “-gauche” with energy difference of only +3.4 kJ/mol (local minimum) with respect to the “trans” conformation. They are also quite stable because they are separated from the “trans” conformation by high 12.6 kJ/mol barriers. In Fig. 3, which shows the energy diagram of hindered internal rotation in butane, the individual conformations are characterized by dihedral angle Φ between the plane formed by the first, second, and third C atoms and that formed by the second, third, and fourth C atoms in the polyethylene chain: “cis,” $\Phi = 0^\circ$; “+gauche,” $\Phi = 60^\circ$; “trans,” $\Phi = 180^\circ$; and “-gauche,” $\Phi = 300^\circ$. The authors considered only three conformations and used statistical thermodynamics to evaluate the partition function and the average conformational characteristics of the ensemble. It may seem that the use of only three stable conformations of the part of

Fig. 3 Schematic energy diagram of hindered internal rotation in butane



the chain containing four C atoms instead of a spectral continuum of a number of conformations depending on the dihedral angle drastically reduces the number of states in the evaluation of the average values of the ensemble. However, the total number of all the considered conformations is 3^{N-1} , which for N ca. 10^3 – 10^5 yields astronomically high values. The number of possible conformations is in fact less than 3^{N-1} , because the “+g –g” and “–g +g” arrangements of two successive four-member parts of the chain, i.e., C atoms i to $(i+4)$ and $(i+1)$ to $(i+5)$, yield the cyclopentane structure and the next C atom $(i+6)$ would overlap with atom i . Therefore, the +g–g and –g+g arrangements are not allowed, and the corresponding interaction energy is $u(+g-g) = u(-g+g) = \infty$.

Inherently stiff chains which contain multiple bonds, bulky pendant groups, etc., do not obey the predictions of the models developed for flexible chains. They form expanded ellipsoidal or rodlike conformations, depending on the conformational rigidity. The behavior of semiflexible chains can be described by the “wormlike chain” model (WLC) developed by Kratky and Porod [31]. We will neither describe this model nor analyze its predictions, but one conformational characteristic of semiflexible chains based on this model, called the “persistence length,” will be briefly mentioned at the end of this chapter. Its physical meaning will be explained and discussed in relation to the behavior of polyelectrolytes, because electrostatic interactions induce an additional stiffening effect in the chain and the highly charged flexible chains thus behave as fairly stiff ones.

The Rouse and the Zimm models are two classical models developed for the description of chain dynamics in the mid-1950s. In addition to dynamic characteristics, they also provide information on the conformational behavior of flexible chains. The Rouse model treats the diffusion of the chain as a collective motion of beads of the same mass connected by elastic springs under the action of randomly fluctuating thermal forces and drag forces [32]. This model neglects both the excluded volume effect and hydrodynamic interactions. It provides correct scaling of size characteristics, but overestimates the decrease in the diffusion coefficient of the chain center of gravity, D , with the length of the chain (number of beads N) predicting the dependence $D \propto 1/N$. The Zimm model [33] is more accurate and assumes both hydrodynamic interactions and excluded volume effects. It predicts the scaling of the diffusion coefficient, $D \propto 1/N^{0.588}$, which is in good agreement with experimental data on self-avoiding chains. Both models neglect solvent effects and the effects of the chemical structure, and hence they predict that the motion of the whole chain can be described by universal formulas, i.e., it depends only on the molar mass of the solvent and friction of the continuous medium in which the chain is immersed (i.e., only on the bulk solvent viscosity). This is a simplification, but the derived formulas describe the dynamic behavior of dilute solutions of nonpolar polymers in nonpolar solvents reasonably well.

To summarize the part devoted to the general behavior of nonpolar polymers in organic solvents, we would like to mention that both linear chains and those with more complicated molecular architectures (stars, brushes, copolymers, etc.) have been intensely studied experimentally, theoretically, and by computer simulations, and their properties are now well understood. The message we would like to convey

is that the fundamental features of the behavior can mostly be adequately explained and understood at a semiquantitative level using the arguments of the simple classical theories outlined above. In the next part, we will concentrate on the more complex and less well-understood conformational and ionization behavior of polyelectrolytes in aqueous media, but would first like to add several general comments on concentrated polymer solutions and polymer melts without going to details.

2 Comments on the Differences Between Dilute and Concentrated Solutions

In dilute solutions, individual polymer chains are relatively far apart and form separated random coils. They move randomly and come into contact from time to time, but are well separated most of the time. The density of the segments, which is proportional to $N^{-1/2}$ in ϑ -solvents, is in fact quite low—it is only several vol.% in most real systems, i.e., the coils are very loose and fairly expanded fractal objects, and the domain of the coil contains a high solvent excess. Good solvents interact favorably with polymer segments, solvate them, and swell the chain—the chain domain expands, and the density of the segments decreases, while the chain contracts in poor solvents. Strictly speaking, dilute polymer solutions are microheterogeneous—they contain separate coil domains immersed in bulk solvent. In a mixture of a good and poor solvents, different interactions (favorable vs. unfavorable) lead to preferential solvation of the chain by the good solvent component, and, in this case, the solvent composition in the domain of the coil may differ from the bulk.

If the concentration increases and the loose coils completely fill the whole volume, they mutually touch and later start to overlap. The “concentration of the first overlap,” c^* , separates the regions of dilute and semi-dilute solutions. With a further increase in concentration, the chains interpenetrate, and the viscosity of the polymer solution increases tremendously. However, this does not mean that the dimensions of the individual chains change very much. Because the chains are loose fractal objects, their segments can easily mutually interpenetrate. In concentrated solutions and in polymer melts, the chains are, on average, uniformly intermixed, and, in contrast to dilute solutions, the solution is homogeneous, but the chains still form random coils. Flory predicted theoretically that the dimensions of polymer coils in an amorphous bulk polymer (which behaves as a very viscous “liquid” above the glass transition temperature) are the same as in a dilute solution of a ϑ -solvent [9]. He explained his hypothesis by the following arguments: In bulk polymers, there exists only one type of interaction between polymer segments (which emulates the situation in a good solvent; there is no difference in interactions, and hence χ is theoretically zero), but the trial chain under consideration is squeezed by neighboring chains. This trial chain fills the space delimited by its coil

domain partially by its own segments, which affect the conformations of neighboring chains. The concentration of their segments in this particular place is lower, and the concentration gradient of their segments (i.e., of their chemical potential) generates a force (analogous to that which would cause diffusion in an inhomogeneous solution) which compresses the trial chain to dimensions corresponding to θ -conditions. This assumption was later demonstrated experimentally by small-angle X-ray scattering (SAXS) and small-angle neutron scattering (SANS). In the first case [34], a homogeneous melt containing a significant excess of regular polystyrene and a low fraction of its derivative containing one $-\text{COOH}$ group at the end of the chain (converted in the $-\text{COO}^- \text{Ag}^+$ salt) was prepared at a fairly high temperature—well above the glass transition temperature. Both polymers are compatible, i.e., they mix easily ensuring homogeneous intermixing. However, their scattering power for X-rays differs because the presence of heavy Ag^+ ions increases the scattering power of the minority component. Therefore, the mixture can be studied by small-angle X-ray scattering (SAXS). From the scattering point of view, the mixture behaves as a solution of “optically modified” polystyrene in unmodified polystyrene. Because the so-called contrast, i.e., the difference in the scattering power of the components, can be estimated independently, the characteristics of the dissolved (minority) polymer, such as its molar mass, radius of gyration, etc., could be estimated. For a given molar mass of the modified PS, the measurement yielded a value of the radius of gyration that nicely corresponded to that in a dilute solution in a θ -solvent. When viewed from the perspective of later discoveries, this study is slightly problematic, because the presence of ions in a nonpolar polymer matrix can provoke their aggregation and formation of ion clusters (known from later studies of ionomers), which could have influenced the data analysis. However, experimental data suggest that the low fraction of modified polystyrene prevented the formation of ion clusters and the measurement yielded the characteristics of the individual modified chains. SANS was also later used by Cotton et al. [35] and by Kriste et al. [36]. Cotton studied deuterized polystyrene in hydrogenated polystyrene, and Kriste investigated deuterized poly(methyl methacrylate) in the hydrogenated polymer. As deuterium and hydrogen atoms differ strongly in their ability to scatter neutrons and the hydrogenated and deuterized polymer chains of the same chemical structure are fully compatible, both research groups obtained good-quality data and provided persuasive proof of the Flory prediction.

3 Polyelectrolyte Chains

The chains of polyelectrolytes (PEs) contain charged groups. PEs can be divided in two classes: Those with permanently charged groups, e.g., sulfonated polystyrene, are called strong or “quenched” polyelectrolytes. The term “quenched” PE reflects the fact that the positions of the charges are fixed (predetermined by the synthesis). Weak or “annealed” PEs contain ionizable groups that can dissociate in polar

solvents, leaving electric charges on the chain and releasing small mobile counterions in the bulk solvent. In contrast to quenched PE, both the ionization (number of charges on the chain) and the positions of the individual charges are not constant, but depend on the external conditions (pH, temperature, ionic strength). Discrete charges appear and disappear at different positions via reversible association/dissociation processes with a relatively high frequency, and because close approach of charges of the same sign is energetically unfavorable, the spatial distribution of charges is correlated with instantaneous chain conformations and fluctuates (it is an “annealed variable” which gave rise to the term annealed PEs).

Upon dissolution of PEs in polar solvents (most often water), a great majority of the counterions escape into the bulk solvent, which increases the entropy of the system and the thermodynamic stability of PE solutions. However, a certain fraction of them concentrate close to the PE chain and screen (partially neutralize) the multiple charge of the macro-ion. If the linear charge density along the chain exceeds a certain critical value, some counterions actually condense on the chain (Manning condensation) [37–39]. The condition for the onset of the Manning condensation requires that the dimensionless Coulomb coupling strength $\Gamma = \lambda_B/l_{ch}$ be equal to 1. Here, l_{ch} is the linear distance between charges in the chain, and λ_B is the Bjerrum length ($\lambda_B = e^2/(4\pi kT) \approx 0.7$ nm in water; this is the distance between the elementary charges at which the Coulomb interaction energy is the same as the energy of thermal motion), e is the elementary charge, k is the Boltzmann constant, and T is the temperature. Because charges of the same sign on the chain are never fully compensated at short distances by counterions, the highly charged chains adopt stretched conformations. Electric charges on the chain are separated as much as possible, which lowers the spatial charge density and causes electrostatic repulsion. An intrinsically flexible linear PE thus behaves as an effectively stiff chain, because the effective chain flexibility is affected and strongly reduced by electrostatic forces (depending on the charge density and ionic strength of the bulk solution). However, in addition to the direct electrostatic effect, there is a second important reason for stretching the chain. Stretched conformations provide a larger volume for constrained motion of “bound” counterions (which compensate the macro-ion charge) along the chain, which does not reduce their translational entropy (and the overall entropy of the system) as much as in collapsed conformations.

The behavior of an overwhelming majority of practically important PEs in aqueous media is significantly affected by the fact that they contain a fairly hydrophobic backbone (e.g., hydrocarbon chain) and their solubility in aqueous media is due to the presence of charges, either on the chain or on pendant electrolyte groups. In many cases, the presence of pendant ionizable groups (which are usually hydrophilic) weakens the hydrophobicity of the chain, which becomes amphiphilic at short distances. For example, the poly(methacrylic acid), PMAA, is well soluble at high pH values, when the carboxylic groups are highly ionized, but is still fairly well soluble in water at low pH values, where the pendant carboxylic groups are not dissociated. However, the parent poly(isopropylene) backbone, from which PMMA can be derived by attaching a pendant $-\text{COOH}$ group at each monomer unit, is an

extremely hydrophobic water-insoluble polymer. In contrast to PMAA, unionized poly(2-vinylpyridine) is fairly hydrophobic and insoluble in neutral buffers, but it is well soluble in acidic media (below pH 5) when the nitrogen atom is protonated and charged. To summarize this paragraph, water is a thermodynamically bad solvent for most PEs.

Experimental studies of PS in poor solvents began in the early 1950s with the paper by Katchalski [40]. Early studies employing viscometry and calorimetry were performed on PMAA and alternating copolymers containing electrolyte and non-polar hydrophobic monomer units in aqueous buffers [40–43]. The most important achievements were made by Strauss et al. [44–46], Morawetz et al. [47–50], and Ghiggino et al. [51]. It was recognized that the behavior of PMAA differs from that of less hydrophobic PEs, such as poly(acrylic acid), PAA. At that time, PMAA was usually described as a polyelectrolyte similar to polysoaps. Ghiggino was the first to propose the “hypercoiling model” specifically for PMAA on the basis of fluorescence studies more than 10 years before a similar Dobrynin “necklace of pearls model” [52] became a widely used scheme for interpreting the conformational behavior of PEs with hydrophobic backbone in aqueous media.

In the following chapters of this book, we will discuss fluorescence measurements performed mainly on PE solutions in thermodynamically poor solvents. Therefore, the behavior of PEs in poor solvents is our main sphere of interest, but we will first mention the classical Kuhn treatment of polyelectrolytes in ϑ -solvents [53]. The potential energy of a polyelectrolyte chain in a given conformation (described by a set of \mathbf{r}_i position vectors of segments) can be written within the framework of the mean-field Debye–Hückel (DH) theory [54] as a sum of three contributions: the energy corresponding to (i) the entropic elasticity of harmonic bonds, U_1 , with bond lengths l , which connect the monomers in the polymer chain. This contribution depends on the set of all position vectors, $\{\mathbf{r}_i\}$

$$U_1(\{\mathbf{r}_i\}) = \frac{3kT}{2l^2} \sum_{i=1}^{N-1} (\mathbf{r}_{i+1} - \mathbf{r}_i)^2 \quad (4)$$

(ii) the screened electrostatic Coulomb (Yukawa) interaction potential, U_2 , between all monomers bearing charges q_i and q_j

$$U_2(\{\mathbf{r}_i\}) = kT \sum_{i=1}^N \sum_{j<i} \frac{\lambda_B q_i q_j}{|\mathbf{r}_i - \mathbf{r}_j|} \exp(-\kappa |\mathbf{r}_i - \mathbf{r}_j|) \quad (5)$$

and (iii) the short-range contribution of dispersion forces, U_3 , which can be expressed using, e.g., the Lennard-Jones potential, $u_{LJ}(r)$, which reasonably approximates the short-range interaction between nonpolar spherical molecules by a power function of their distance r

$$u_{\text{LN}}(r) = 4\epsilon \left[\left(\frac{\sigma}{r} \right)^{12} - \left(\frac{\sigma}{r} \right)^6 \right] \quad (6)$$

At the level of the DH approximation, the interaction energy of segment–counterion interactions and added salt–ion interactions does not appear explicitly in the formula and enters indirectly via the concentration dependence of the Debye screening length, $r_{\text{D}}^{-2} = \kappa^2 = 4\pi\lambda_{\text{B}} \sum c_s q_s^2$, where c_s and q_s are the concentrations of small ions of the s type and their valences, respectively. Kuhn used a model of the chain without short-range interactions (i.e., without U_3) and minimized the expression for the free energy of the system. The crucial rough approximation which he used consisted in the fact that he evaluated the conformational part neglecting the interactions, and the interaction part neglecting the chain connectivity assuming that (i) the charged monomers are distributed uniformly in the chain volume. Taking into account the experimental findings, he further assumed that (ii) electrostatic interactions lead to unidirectional elongation of the chain conformations. He actually postulated that the PE chain adopts the shape of a rotationally symmetrical elongated ellipsoid with one perturbed (electrostatically affected) longitudinal size R_{E}^{P} and two unperturbed perpendicular sizes, $R_{\text{E}}^{\text{UP}} = lN^{1/2}$. For R_{E}^{P} , he obtained the relationship

$$R_{\text{E}}^{\text{P}} = lNu^{1/3}f^{2/3} \left[\ln \left\{ eN(uf^2)^{2/3} \right\} \right]^{1/3} \quad (7)$$

where u is the “interaction parameter” defined as $u = \lambda_{\text{B}}/l$ and f denotes the fraction of charged monomers.

The behavior of PE chains can be analyzed in more detail by the scaling approach based on the concept of thermal and electrostatic blobs. The blob theory assumes that, on small length scales shorter than the “correlation length” ξ_{T} (called also the “blob size”), the energy of random thermal motion counterbalances the excluded volume effect of segments, and short parts of the chain behave as ideal chains. Therefore, it holds that $\xi_{\text{T}}^2 = g_{\text{T}}l^2$, where g_{T} is the number of segments per blob and l is the bond (segment) length. At longer lengths, the effect of the excluded volume dominates the conformational behavior, and the chain behaves as a self-avoiding walk. Taking into account the balance of forces, the size of the thermal blob can be related to the Flory–Huggins interaction parameter, $\xi_{\text{T}} = l/(1 - 2\chi)$. The electrostatic blob is an extension of the blob concept. The assumption that the conformations inside the electrostatic blob are not perturbed by electrostatic interactions with the corresponding balance of forces yields the relationship between the “interaction parameter” u , the fraction of charged units f , and the parameters that characterize the blob, i.e., the number of segments, $g_{\text{E}} = (uf^2)^{-2/3}$, and the electrostatic correlation length (blob size), $\xi_{\text{E}} = l(uf^2)^{-1/3}$. Application of the scaling approach to the problem of PEs predicts that, on length scales larger than ξ_{E} , the electric charges on the PE chain generate a force which nonuniformly deforms the chain in one direction. This leads to a roughly uniaxial arrangement of electrostatic

blobs in a “string of blobs.” The size of the blobs is not constant, but increases toward both ends of the chain. This result is not surprising, because the central section of the chain experiences stronger electrostatic repulsion than the ends of the chain. What is slightly surprising is the finding that the evaluation of the elongated chain size R_E^P yields an identical result to the simple approximate Kuhn model.

Now, we will discuss the behavior of quenched PEs in poor solvents. Experimental studies show that the effective solvent quality depends on a number of factors, namely, the degree of ionization of PE and the ionic strength. A poor solvent for a neutral chain can be a good solvent for the same charged polymer. Sparsely ionized PEs have only low solubility and form compact globular conformations in bad solvents (aqueous buffer), while a polymer of the same chemical nature dissolves well when its chain is strongly ionized and forms a fairly stretched conformation. We should recall that the variable ionization of a quenched PE requires the incorporation of different fractions of permanently charged comonomers in different chains during synthesis, and hence the chemical compositions of chains with different degrees of ionization are not identical. The first attempt to theoretically treat the behavior of quenched PEs in poor solvents was made by Khokhlov [55, 56]. He predicted that a spherically symmetrical globular conformation would deform with increasing charge and would form a prolate ellipsoid. A substantially more detailed description, which is at present generally accepted, was published by Dobrynin, Rubinstein, and Obukhov in 1996 [52]. They combined the scaling approach and Monte Carlo simulation and showed that the transition from the globular to the stretched conformation proceeds as a cascade transition via a series of “pearl necklace” structures (globules formed by collapsed parts of the chain interconnected by relatively short stretched parts) with increasing numbers of pearls of decreasing sizes. The proposed necklace concept was inspired by earlier theoretical works by Kantor and Kardar [57], who explained the formation of globules within one chain by the same physical arguments as used by Rayleigh in 1882 when he studied the instability of charged oil droplets [58]. When an oil droplet is charged, the charge spreads over its surface. Discrete elementary charges of the same sign aim at expanding the surface, because they try to be as far as possible from each other. The corresponding electrostatic potential of repulsive forces is proportional to the square of the total charge and to the reciprocal (average) distance between the charges $\langle r^{-1} \rangle$, which is proportional to the radius of the droplet, R , i.e., $\approx Q^2/(\epsilon R)$, ϵ is the dielectric permittivity. The surface energy (proportional to γR^2 , γ is the surface tension) tries to minimize the surface and preserve the spherical shape. When the charge increases and exceeds the critical value, at which both terms are equal, the “mother” droplet splits into two smaller “daughter” droplets because the Gibbs energy of the two “daughter” droplets is lower than that of the original “mother” droplet. As both “daughter” droplets contain electric charges of the same sign, they mutually repel and move away from each other.

The formation of pearls on the chain can be explained by analogous arguments. In a poor solvent, minimization of the number of unfavorable interactions between

non-ionized polymer segments and solvent molecules leads to a compact globular arrangement with minimum surface-to-volume area. When the charge on the chain increases, or the solvent quality improves and the effective surface tension decreases, the condition for Rayleigh instability is reached, and the globular conformation splits into two smaller globules. The globules cannot separate due to the chain connectivity and are kept together at a certain distance by a relatively short, albeit fairly stretched part of the chain. From a practical point of view, study of a system with “continuously” increasing charge on the chain assumes synthesis of a series of tailor-made PE samples with increasing numbers of charged groups incorporated into the chain, which is very demanding. It is much easier to vary the solvent quality by changing the temperature, but the range of solvent qualities for temperatures preventing temperature-induced decomposition of the polymer chains is fairly limited. If the chain charge (or temperature) continues to increase, a series of conformation transitions (splitting of globules) will gradually occur. Based on the scaling approach, Dobrynin et al. derived the following formula for the critical charge fraction f_{crit} which corresponds to the Rayleigh instability:

$$f_{\text{crit}} = [|\tau|/(N u)]^{1/2} \quad (8)$$

where $\tau = (1-\vartheta/T)$, ϑ is the theta temperature and N is the total number of segments (monomer units). Theoretical description of the “pearl necklace” structure is relatively complicated because it does not reflect only the Rayleigh instability but also has to take into account other factors. The two charged globules electrostatically repel each other, increasing the energy of the pearl structure. The formation of a string connecting two globules requires that some monomers that were originally hidden inside the large “mother” globule now be exposed to the poor solvent, which is energetically unfavorable. In addition, the string contributes to the overall free energy of the system by its elastic and electrostatic parts. By minimizing the free energy, the authors derived the appropriate formulas for all the relevant parameters that characterize the pearl necklace structure of a chain consisting of n_b globules with size (diameter) D_b containing m_b monomers each. The globules are connected by strings, each having m_{st} monomers, and the total number of monomer units in the PE chain is N . Here, we reproduce only the formula for the total length of the necklace conformation, L_{nec} :

$$L_{\text{nec}} = N l f \sqrt{\frac{u}{|\tau|} \ln \left(\frac{N u f^2}{|\tau|} \right)} \quad (9)$$

where $\tau = (1-\vartheta/T)$.

The above-described hypothesis was confirmed by many Monte Carlo and molecular dynamics simulations and also by a number of experimental techniques [59–76]. Because the globules are fairly dynamic structures which “move” along the chain, the number of persuasive direct experimental proofs is still limited.

Nevertheless, the above “pearl necklace” scheme is now a generally accepted scheme for the conformational behavior of PEs in poor solvents.

The behavior of annealed PEs in poor solvents is more complex than that of quenched PEs. The probability of dissociation of a particular ionizable group depends, among other factors, on its distances from already ionized neighbor groups. It should be borne in mind that the simultaneous dissociation of two closely spaced ionizable groups is unfavorable, which can be documented by the low ratio of the second-to-first step dissociation constants in oxalic acid, K_2/K_1 approx. 10^{-3} . Hence, the distribution of annealed charges along the chain and its fluctuations are closely related to the instantaneous chain conformations. Therefore, it is not surprising that recent theoretical and computer studies predict different conformational behavior than for quenched PEs.

Conformational transitions in annealed PE solutions have been studied theoretically by Raphael and Joanny [77]. They predicted that annealed PEs should undergo a sudden first-order transition from a highly charged expanded conformation to a collapsed and very little ionized one with a pH-controlled change (decrease) in the degree of ionization. Recent semi-grand canonical Monte Carlo (MC) simulations performed at a constant chemical potential of the charged species indicate some ambiguity and do not support a first-order transition. Several authors observed a first-order transition for annealed PEs only in very poor solvents, while they observed the formation of pearls in marginal poor solvents (close to θ -conditions) [68]. Other authors claim that pearl necklace structures are also formed in very poor solvents [63]. At present, the debate concerning the transition from the expanded to the collapsed state is still ongoing, but most researchers believe (or incline to the opinion) that a cascade of pearl necklace transitions proceeds in a broad range of solvent qualities.

4 Comments on Computer Studies of Polymer Conformations and Dynamics

Computer studies (both Monte Carlo and molecular dynamic simulations) have become a very powerful tool for studying the conformational and dynamic behavior of polymer chains. They can be used for testing the predictions of theoretical models concerning the equilibrium properties and moreover they provide information on dynamic characteristics, e.g., on instantaneous fluctuations of chain shapes which is important because most experimental techniques (e.g., scattering techniques) yield the ensemble-average characteristics only. Large numbers of studies have been performed on neutral chains—not only on linear ones but also on stars, combs, etc. [78–85]. The most important advances in understanding the behavior of polyelectrolytes have been made mainly thanks to computer studies. As already mentioned, quenched PEs have been studied both by Monte Carlo [86–89] and by molecular dynamics simulations [59, 63, 71, 73, 87, 90]. Simulation of annealed

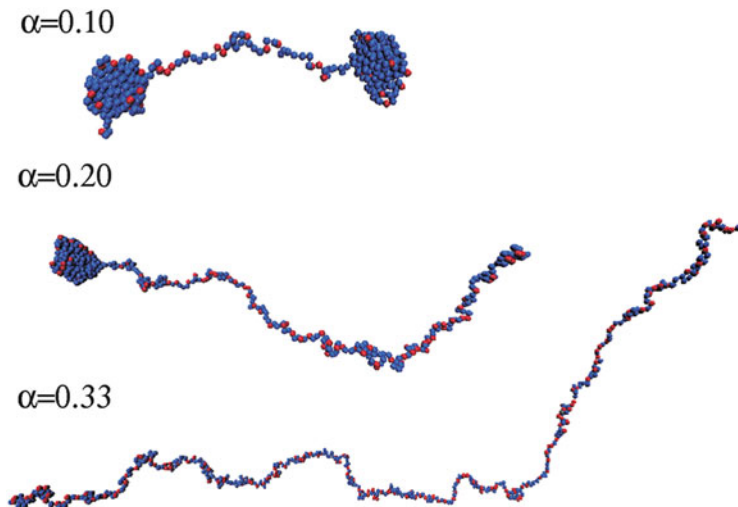


Fig. 4 Simulation snapshots of chain conformations in a bad solvent for three degrees of ionization α . Adapted with kind permission from Collection of Czechoslovak Chemical Communications 73, 2008, 439–458, figure 4, [93]. Copyright 2011

PEs is a very complex and delicate problem, because correct treatment of the dissociation equilibrium at constant pH assumes constant chemical potential of the hydrated protons and other small ions.

So far, almost all computer studies of annealed PEs have been performed by grand canonical Monte Carlo methods (or by reaction ensemble MC), because these simulation variants can treat variable dissociation relatively easily keeping the chemical potentials of small charged species constant [59, 63, 68, 69, 91, 92]. Current molecular dynamics (MD) studies usually use the degree of ionization as an input parameter and cannot correctly treat systems with “mobile charges.” However, an interesting MD attempt for annealed PEs was published by Kosovan et al. [93]. The authors combined common molecular dynamics and Monte Carlo methodology. They incorporated a MC exchange of the positions of charges in the chain (submitted to the Metropolis acceptance criterion) [94] in a MD run which made it possible to emulate the appearance and disappearance of mobile charges in different positions on the chain. The authors analyzed the behavior of annealed chains under the condition of a fixed overall degree of ionization using several ensemble-averaged functions: the probability of ionization of monomer units $P(q, i)$ as a function of their position (running number i) in the chain contour and the average bond cosines, i.e., by $\langle \mathbf{r}_{i+1} \cdot \mathbf{r}_i \rangle / (|\mathbf{r}_{i+1}| \cdot |\mathbf{r}_i|)$, where \mathbf{r}_i is the bond vector i . The ensemble average cosine of the angle between two successive bonds i and $(i + 1)$ is a good indicator of the local behavior: It equals zero (or low) in stretched parts of the chain and can increase up to 0.5 in coiled globular parts of the chain. Simulation data for a chain with 500 unimer units and three overall degrees of ionization $\alpha = 0.1, 0.2$, and 0.33 in a bad solvent with the reduced Lennard-Jones interaction parameter $\epsilon = 1.0$ are shown in Fig. 4. Figure 5 presents the schematics

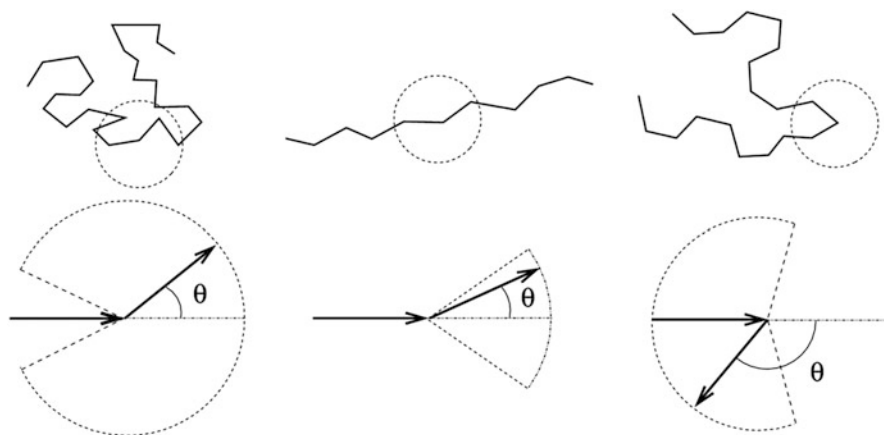


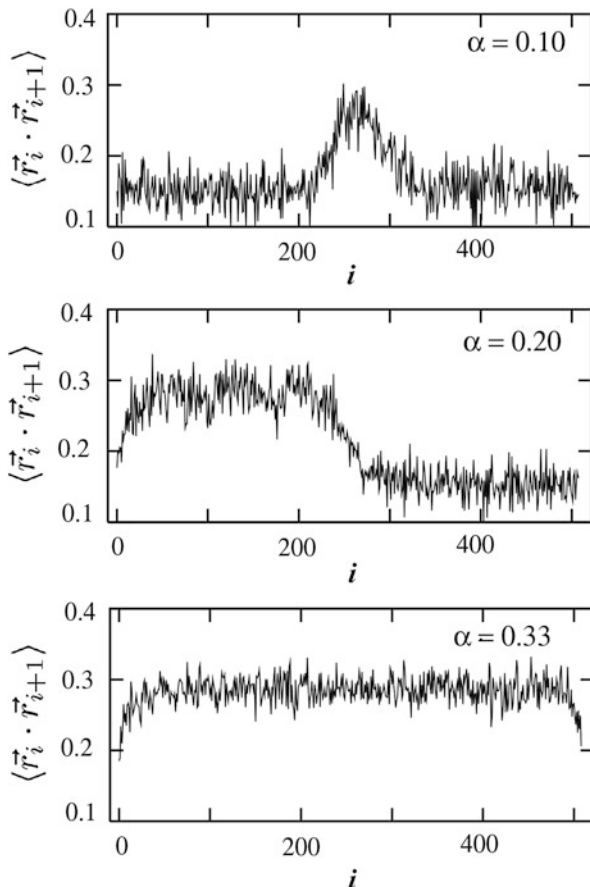
Fig. 5 Schematic illustration of the possible values of bond-angle cosines. Adapted with kind permission from Collection of Czechoslovak Chemical Communications 73, 2008, 439–458, figure 6, [93]. Copyright 2011

explaining the evaluation of bond-angle cosines, Fig. 6 depicts the distribution functions of bond-angle cosines as functions of the position of monomer units in the polymer chain for the above overall degree of ionization, and Fig. 7 shows the probability of ionization of individual beads. Note that $\varepsilon = 0.34$ describes the ϑ -temperature [70]. The data show that the chain forms a pearl necklace structure and the units inside compact globules are considerably less ionized than those exposed to the solvent in the stretched part of the chain.

5 The Persistence Length

In the part devoted to neutral polymers, we mentioned that semiflexible and stiff chains do not obey the behavior predicted by the Kuhn model. Restricted flexibility of the chain can be caused by the presence of stiff units with multiple bonds or bulky pendant groups, but it can be a result of external conditions or stimuli. In the preceding part, it was explained in detail that repulsive interactions together with entropic forces increase the stiffness of PE chains. Hence, a sudden pH change can be used as a stimulus affecting the stiffness of annealed PE chains. The properties of semiflexible polymers are usually treated at the level of the wormlike chain (WLC) model developed by Kratky and Porod [31]. The “persistence length,” l_p , is an important parameter strongly related to the WLC model and has been used as the most common characteristic of chain flexibility—in both theoretical and experimental studies. It is used to describe orientational correlations between successive bond vectors in a polymer chain in terms of the normalized orientation correlation function, $C(s) = \langle \mathbf{r}_i \cdot \mathbf{r}_{i+s} \rangle$. For the WRC model, this function decays exponentially:

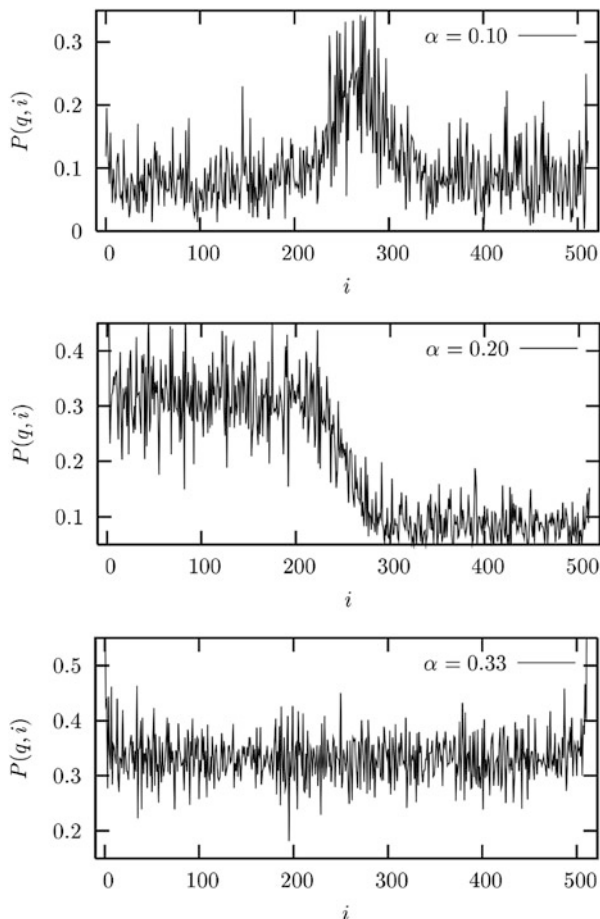
Fig. 6 Average bond-angle cosines as functions of the position of the monomer unit in the polymer chain for the polymer in a bad solvent for three degrees of ionization α . Adapted with kind permission from Collection of Czechoslovak Chemical Communications 73, 2008, 439–458, figure 7, [93]. Copyright 2011



$$C(s) = \exp\left(\frac{-s}{l_P}\right) \quad (10)$$

and the persistence length l_P is related to the bending modulus κ of the chain by $l_P = \kappa/kT$. The persistent length l_P is the length at which the chain “forgets” the orientation of its first segment, i.e., at distances shorter than l_P , short parts of the chain behave like an elastic rod, while at longer distances, the conformational properties can be described statistically by a random walk model. Equation (10) actually describes the rate of decay of the ensemble average cosine of the angle between the orientations of the first and the s -st segment (generally between the n -st and $(n+s)$ -st segment) in the chain. From the geometrical point of view, l_P equals the average projection of the end-to-end vector on the tangent to the chain contour at chain end at the limit of infinite length. For the freely jointed chain (Kuhn model), the persistence length is only one half of the segment length, $(1/2)l$.

Fig. 7 The probability of charging of individual monomer units $P(q,i)$ for the polymer in a bad solvent as a function of their position in the chain, i , for three degrees of ionization α . Adapted with kind permission from Collection of Czechoslovak Chemical Communications 73, 2008, 439–458, figure 9, [93]. Copyright 2011



The effect of electrostatics on the persistence length of polyelectrolytes has been studied by a number of researchers. The first theoretical model was developed independently by Odijk [95] and by Skolnick and Fixman [96]. They expressed the total persistence length, l_p , as the sum of the natural persistence length, l_0 , and the electrostatic persistence length, l_E , i.e., $l_p = l_0 + l_E$. For long chains, they obtained the following formula:

$$l_E = (\alpha N)^2 \lambda_B \lambda_D^2 / 4 \quad (11)$$

where λ_B is the Bjerrum length, λ_D is the Debye screening length, N is the number of monomer units, and α is the normalized linear charge density on the chain. Later, Khokhlov et al. [97] reformulated the problem for a chain of blobs and also obtained the scaling of l_B on λ_D^2 . However, there is a strong controversy about the dependence of l_B on λ_D . This problem has been amply studied by computer

simulations [98–100]. Computer simulations suggest that the correlation function of the segment orientations in PE chains cannot be expressed as a single exponential function. The fact that the short-range behavior is dominated by intrinsic stiffness, while the long-range part of orientational correlations is controlled by electrostatics, and that there exists a crossover between these two regimes were suggested originally by Barrat and Joanny [101] and later confirmed by simulations [102]. Gubarev et al. [103] proposed the double-exponential decay of $C(s)$:

$$C(s) = B \exp\left(-\frac{s}{l_1}\right) + (1 - B) \exp\left(-\frac{s}{l_2}\right) \quad (12)$$

where l_1 and l_2 are two different decay lengths. Manghi and Netz [104], Dobrynin et al. [103], and others [105] studied the problem in detail and proposed the relation between l_i , l_0 , and l_E . They also confirmed that the dependence of l_B on λ_D is more complex than that proposed by Odijk and Skolnick with Fixman.

Acknowledgment This work was supported by the Czech Science Foundation (Grants P106-12-0143 and P106-15-19542S). The authors would like to thank Lucie Suchá and Karel Šindelka for their help with graphics.

References

1. Rubinstein M, Colby R (2003) *Polymers physics*. Oxford University Press, Oxford
2. Sperling LH (2005) *Introduction to physical polymer science*. Wiley, Hoboken, NJ
3. Munk P (1989) *Introduction to macromolecular science*. Wiley, New York
4. Doi M, See H (1996) *Introduction to polymer physics*. Clarendon, Oxford
5. Kawakatsu T (2004) *Statistical physics of polymers: an introduction*. Springer, Berlin
6. Lodge TP, Muthukumar M (1996) Physical chemistry of polymers: entropy, interactions, and dynamics. *J Phys Chem* 100:13275–13292. doi:[10.1021/Jp960244z](https://doi.org/10.1021/Jp960244z)
7. Freire JJ (1999) Conformational properties of branched polymers: theory and simulations. *Branched Polym II* 143:35–112
8. Huggins ML (1942) Theory of solutions of high polymers. *J Am Chem Soc* 64(7):1712–1719. doi:[10.1021/ja01259a068](https://doi.org/10.1021/ja01259a068)
9. Flory PJ (1949) The configuration of real polymer chains. *J Chem Phys* 17(3):303–310. doi:[10.1063/1.1747243](https://doi.org/10.1063/1.1747243)
10. Flory PJ (1970) Thermodynamics of polymer solutions. *Discuss Faraday Soc* 49:7
11. Flory PJ (1945) Thermodynamics of dilute solutions of high polymers. *J Chem Phys* 13 (11):453–465. doi:[10.1063/1.1723978](https://doi.org/10.1063/1.1723978)
12. Flory PJ (1953) *Principles of polymer chemistry*. Cornell University Press, Ithaca, NY
13. Flory PJ, Krigbaum WR (1951) Thermodynamics of high polymer solutions. *Annu Rev Phys Chem* 2:383–402. doi:[10.1146/annurev.pc.02.100151.002123](https://doi.org/10.1146/annurev.pc.02.100151.002123)
14. Flory PJ (1942) Thermodynamics of high polymer solutions. *J Chem Phys* 10(1):51–61
15. Huggins ML (1942) Some properties of solutions of long-chain compounds. *J Phys Chem* 46 (1):151–158. doi:[10.1021/j150415a018](https://doi.org/10.1021/j150415a018)
16. Teraoka I (2002) *Polymer solutions: an introduction to physical properties*. Wiley, New York
17. Yamakawa H (1971) *Modern theory of polymer solutions*. Harper & Row, New York
18. Brandrup J, Immergut EH, Grulke EA, Abe A, Bloch DR (1999) *Polymer handbook*, vol 89. Wiley, New York

19. Wanka G, Hoffmann H, Ulbricht W (1994) Phase-diagrams and aggregation behavior of poly (oxyethylene)-poly(oxypropylene)-poly(oxyethylene) triblock copolymers in aqueous-solutions. *Macromolecules* 27(15):4145–4159. doi:[10.1021/ma00093a016](https://doi.org/10.1021/ma00093a016)
20. Attwood D, Collett J, Tait C (1986) Photon correlation studies on the micelles of a poly (oxyethylene)-poly (oxypropylene)-poly (oxyethylene) block copolymer in aqueous solution. In: *Surfactants in solution*. Springer, pp 419–426
21. Kuhn W, Grun F (1942) Relationships between elastic constants and stretching double refraction of highly elastic substances. *Kolloid-Z* 101:248
22. James HM, Guth E (1943) Theory of the elastic properties of rubber. *J Chem Phys* 11 (10):455–481
23. Rudnick J, Gaspari G (1987) The shapes of random-walks. *Science* 237(4813):384–389. doi:[10.1126/science.237.4813.384](https://doi.org/10.1126/science.237.4813.384)
24. Tanford C, Huggins ML (1962) Physical chemistry of macromolecules. *J Electrochem Soc* 109(3):98C
25. De Gennes P-G (1979) *Scaling concepts in polymer physics*. Cornell University Press, Ithaca, NY
26. Binder K (1995) *Monte Carlo and molecular dynamics simulations polymer*. Oxford University Press, New York
27. Flory P, Volkenstein M (1969) *Statistical mechanics of chain molecules*. Wiley, New York
28. Volkenstein MV (1958) The configurational statistics of polymeric chains. *J Polym Sci* 29 (120):441–454. doi:[10.1002/pol.1958.1202912012](https://doi.org/10.1002/pol.1958.1202912012)
29. Lifson S (1959) Neighbor interactions and internal rotations in polymer molecules. 3. Statistics of interdependent rotations and their application to the polyethylene molecule. *J Chem Phys* 30(4):964–967. doi:[10.1063/1.1730136](https://doi.org/10.1063/1.1730136)
30. Nagai K, Ishikawa T (1965) Internal rotation and Kerr effect in polymer molecules. *J Chem Phys* 43(12):4508. doi:[10.1063/1.1696725](https://doi.org/10.1063/1.1696725)
31. Kratky O, Porod G (1949) Rontgenuntersuchung geloster fadenmolekule. *Recueil Des Travaux Chimiques Des Pays-Bas J R Neth Chem Soc* 68(12):1106–1122
32. Rouse PE (1953) A theory of the linear viscoelastic properties of dilute solutions of coiling polymers. *J Chem Phys* 21(7):1272–1280. doi:[10.1063/1.1699180](https://doi.org/10.1063/1.1699180)
33. Zimm BH (1956) Dynamics of polymer molecules in dilute solution—viscoelasticity, flow birefringence and dielectric loss. *J Chem Phys* 24(2):269–278. doi:[10.1063/1.1742462](https://doi.org/10.1063/1.1742462)
34. Krigbaum WR, Godwin RW (1965) Direct measurement of molecular dimensions in bulk polymers. *J Chem Phys* 43(12):4523. doi:[10.1063/1.1696728](https://doi.org/10.1063/1.1696728)
35. Cotton JP, Farnoux B, Jannink G, Strazielle C (1973) Dilute and semidilute solutions—light and neutron-scattering and osmotic-pressure. *J Polym Sci Part C Polym Symp* 42:981–985
36. Kirste RG, Schelten J, Kruse WA (1972) Determination of radius of gyration of poly(methyl methacrylate) in glass state by neutron-diffraction. *Makromol Chem* 162:299
37. Manning GS (1996) Counterion condensation theory constructed from different models. *Physica A* 231(1–3):236–253. doi:[10.1016/0378-4371\(95\)00452-1](https://doi.org/10.1016/0378-4371(95)00452-1)
38. Manning GS (1969) Limiting laws and counterion condensation in polyelectrolyte solutions. I. Colligative properties. *J Chem Phys* 51(3):924. doi:[10.1063/1.1672157](https://doi.org/10.1063/1.1672157)
39. Manning GS (1969) Limiting laws and counterion condensation in polyelectrolyte solutions II. Self-diffusion of the small ions. *J Chem Phys* 51(3):934–938
40. Katchalsky A (1951) Solutions of polyelectrolytes and mechanochemical systems. *J Polym Sci* 7(4):393–412. doi:[10.1002/pol.1951.120070403](https://doi.org/10.1002/pol.1951.120070403)
41. Crescenz V, Delben F, Quadri F (1972) Calorimetric investigation of poly(methacrylic acid) and poly(acrylic acid) in aqueous-solution. *J Polym Sci Part A* 10(2):357. doi:[10.1002/pol.1972.160100215](https://doi.org/10.1002/pol.1972.160100215)
42. Delben F, Quadri F, Crescenz V (1972) Enthalpy of dissociation of poly(methacrylic acid) in aqueous-solution. *Eur Polym J* 8(7):933. doi:[10.1016/0014-3057\(72\)90054-7](https://doi.org/10.1016/0014-3057(72)90054-7)
43. Arnold R (1957) The titration of polymeric acids. *J Colloid Sci* 12(6):549–556. doi:[10.1016/0095-8522\(57\)90060-0](https://doi.org/10.1016/0095-8522(57)90060-0)

44. Strauss UP, Schlesinger MS (1978) Effects of alkyl group-size and counterion type on behavior of copolymers of maleic-anhydride and alkyl vinyl ethers. 2. Fluorescence of dansylated copolymers. *J Phys Chem* 82(14):1627–1632. doi:[10.1021/j100503a011](https://doi.org/10.1021/j100503a011)
45. Strauss UP, Vesnaver G (1975) Optical probes in polyelectrolyte studies. 1. Acid–base equilibria of dansylated copolymers of maleic-anhydride and alkyl vinyl ethers. *J Phys Chem* 79(15):1558–1561. doi:[10.1021/j100582a017](https://doi.org/10.1021/j100582a017)
46. Strauss UP, Vesnaver G (1975) Optical probes in polyelectrolyte studies. 2. Fluorescence-spectra of dansylated copolymers of maleic-anhydride and alkyl vinyl ethers. *J Phys Chem* 79(22):2426–2429. doi:[10.1021/j100589a017](https://doi.org/10.1021/j100589a017)
47. Bednar B, Morawetz H, Shafer JA (1984) Kinetics of the cooperative complex-formation and dissociation of poly(acrylic acid) and poly(oxyethylene). *Macromolecules* 17(8):1634–1636. doi:[10.1021/ma00138a037](https://doi.org/10.1021/ma00138a037)
48. Bednar B, Morawetz H, Shafer JA (1985) Kinetics of the conformational transition of poly(methacrylic acid) after changes of its degree of ionization. *Macromolecules* 18(10):1940–1944. doi:[10.1021/ma00152a024](https://doi.org/10.1021/ma00152a024)
49. Wang YC, Morawetz H (1986) Study of the equilibrium and the kinetics of the fluorescence enhancement on mixing solutions of auramine-o and poly(methacrylic acid). *Macromolecules* 19(7):1925–1930. doi:[10.1021/ma00161a024](https://doi.org/10.1021/ma00161a024)
50. Horsky J, Morawetz H (1988) Kinetics of the conformational transition of poly(methacrylic acid) after a pH jump. 2. Studies of nonradiative energy-transfer. *Makromol Chem* 189(10):2475–2483
51. Ghiggino K, Tan K, Phillips D (1985) *Polymer photophysics*. Chapman and Hall, London
52. Dobrynin AV, Rubinstein M, Obukhov SP (1996) Cascade of transitions of polyelectrolytes in poor solvents. *Macromolecules* 29(8):2974–2979. doi:[10.1021/ma9507958](https://doi.org/10.1021/ma9507958)
53. Kuhn W, Kunzle O, Katchalsky A (1948) Verhalten polyvalenter fadenmolekelionen in losung. *Helv Chim Acta* 31(7):1994–2037. doi:[10.1002/hlca.19480310716](https://doi.org/10.1002/hlca.19480310716)
54. Debye P, Huckel E (1923) The interionic attraction theory of deviations from ideal behavior in solution. *Z Phys* 24:185
55. Dormidontova EE, Erukhimovich IY, Khokhlov AR (1994) Microphase separation in poor-solvent polyelectrolyte solutions—phase-diagram. *Macromol Theory Simul* 3(4):661–675. doi:[10.1002/mats.1994.040030403](https://doi.org/10.1002/mats.1994.040030403)
56. Vasilevskaya VV, Khokhlov AR (1992) Swelling and collapse of polymer gel in polymer-solutions and melts. *Macromolecules* 25(1):384–390. doi:[10.1021/ma00027a059](https://doi.org/10.1021/ma00027a059)
57. Kantor Y, Kardar M (1994) Excess charge in polyampholytes. *Europhys Lett* 27(9):643–648. doi:[10.1209/0295-5075/27/9/002](https://doi.org/10.1209/0295-5075/27/9/002)
58. Rayleigh L (1882) On the equilibrium of liquid conducting masses charged with electricity. *Philos Mag Ser 5* 14(87):184–186. doi:[10.1080/14786448208628425](https://doi.org/10.1080/14786448208628425)
59. Lyulin AV, Dunweg B, Borisov OV, Darinskii AA (1999) Computer simulation studies of a single polyelectrolyte chain in poor solvent. *Macromolecules* 32(10):3264–3278. doi:[10.1021/ma981818w](https://doi.org/10.1021/ma981818w)
60. Liao Q, Dobrynin AV, Rubinstein M (2003) Molecular dynamics simulations of polyelectrolyte solutions: nonuniform stretching of chains and scaling behavior. *Macromolecules* 36(9):3386–3398. doi:[10.1021/ma025995f](https://doi.org/10.1021/ma025995f)
61. Liao Q, Dobrynin AV, Rubinstein M (2006) Counterion-correlation-induced attraction and necklace formation in polyelectrolyte solutions: theory and simulations. *Macromolecules* 39(5):1920–1938. doi:[10.1021/ma052086s](https://doi.org/10.1021/ma052086s)
62. Liu B, Dunweg B (2003) Translational diffusion of polymer chains with excluded volume and hydrodynamic interactions by Brownian dynamics simulation. *J Chem Phys* 118(17):8061–8072. doi:[10.1063/1.1564047](https://doi.org/10.1063/1.1564047)
63. Ulrich S, Laguerie A, Stoll S (2005) Titration of hydrophobic polyelectrolytes using Monte Carlo simulations. *J Chem Phys* 122(9), 094911. doi:[10.1063/1.1856923](https://doi.org/10.1063/1.1856923)

64. Chodanowski P, Stoll S (1999) Monte Carlo simulations of hydrophobic polyelectrolytes: evidence of complex configurational transitions. *J Chem Phys* 111(13):6069–6081. doi:[10.1063/1.479905](https://doi.org/10.1063/1.479905)
65. Uhlik F, Kosovan P, Limpouchova Z, Prochazka K, Borisov OV, Leermakers FAM (2014) Modeling of ionization and conformations of starlike weak polyelectrolytes. *Macromolecules* 47(12):4004–4016. doi:[10.1021/ma500377y](https://doi.org/10.1021/ma500377y)
66. Ou ZY, Muthukumar M (2005) Langevin dynamics of semiflexible polyelectrolytes: rod-toroid-globule-coil structures and counterion distribution. *J Chem Phys* 123(7):074905. doi:[10.1063/1.1940054](https://doi.org/10.1063/1.1940054)
67. Yamaguchi T, Kiuchi T, Matsuoka T, Koda S (2005) Multi-pH Monte Carlo simulation of coil-globule transition of weak polyelectrolyte. *Bull Chem Soc Jpn* 78(12):2098–2104. doi:[10.1246/bcsj.78.2098](https://doi.org/10.1246/bcsj.78.2098)
68. Uyaver S, Seidel C (2004) Pearl-necklace structures in annealed polyelectrolytes. *J Phys Chem B* 108(49):18804–18814. doi:[10.1021/jp0464270](https://doi.org/10.1021/jp0464270)
69. Uyaver S, Seidel C (2009) Effect of varying salt concentration on the behavior of weak polyelectrolytes in a poor solvent. *Macromolecules* 42(4):1352–1361. doi:[10.1021/ma801817j](https://doi.org/10.1021/ma801817j)
70. Micka U, Holm C, Kremer K (1999) Strongly charged, flexible polyelectrolytes in poor solvents: molecular dynamics simulations. *Langmuir* 15(12):4033–4044. doi:[10.1021/la981191a](https://doi.org/10.1021/la981191a)
71. Limbach HJ, Holm C (2003) Single-chain properties of polyelectrolytes in poor solvent. *J Phys Chem B* 107(32):8041–8055. doi:[10.1021/jp027606p](https://doi.org/10.1021/jp027606p)
72. Limbach HJ, Holm C (2001) End effects of strongly charged polyelectrolytes: a molecular dynamics study. *J Chem Phys* 114(21):9674–9682. doi:[10.1063/1.1370077](https://doi.org/10.1063/1.1370077)
73. Limbach HJ, Holm C, Kremer K (2002) Structure of polyelectrolytes in poor solvent. *Europhys Lett* 60(4):566–572. doi:[10.1209/epl/i2002-00256-8](https://doi.org/10.1209/epl/i2002-00256-8)
74. Kosovan P, Kuldova J, Limpouchova Z, Prochazka K, Zhulina EB, Borisov OV (2010) Molecular dynamics simulations of a polyelectrolyte star in poor solvent. *Soft Matter* 6(9):1872–1874. doi:[10.1039/b925067k](https://doi.org/10.1039/b925067k)
75. Kosovan P, Kuldova J, Limpouchova Z, Prochazka K, Zhulina EB, Borisov OV (2009) Amphiphilic graft copolymers in selective solvents: molecular dynamics simulations and scaling theory. *Macromolecules* 42(17):6748–6760. doi:[10.1021/ma900768p](https://doi.org/10.1021/ma900768p)
76. Kosovan P, Limpouchova Z, Prochazka K (2007) Conformational behavior of comb-like polyelectrolytes in selective solvent: computer simulation study. *J Phys Chem B* 111(29):8605–8611. doi:[10.1021/jp072894g](https://doi.org/10.1021/jp072894g)
77. Raphael E, Joanny JF (1990) Annealed and quenched polyelectrolytes. *Europhys Lett* 13(7):623–628. doi:[10.1209/0295-5075/13/7/009](https://doi.org/10.1209/0295-5075/13/7/009)
78. Binder K, Paul W (2008) Recent developments in Monte Carlo simulations of lattice models for polymer systems. *Macromolecules* 41(13):4537–4550. doi:[10.1021/ma702843z](https://doi.org/10.1021/ma702843z)
79. Binder K, Muller M, Virnau P, MacDowell LG (2005) Polymer plus solvent systems: phase diagrams, interface free energies, and nucleation. In: Holm C, Kremer K (eds) *Advanced computer simulation approaches for soft matter sciences I*, vol 173, *Advances in Polymer Science*. Springer, Berlin, pp 1–104. doi:[10.1007/b99426](https://doi.org/10.1007/b99426)
80. Baschnagel J, Binder K, Doruker P, Gusev AA, Hahn O, Kremer K, Mattice WL, Muller-Plathe F, Murat M, Paul W, Santos S, Suter UW, Tries V (2000) Bridging the gap between atomistic and coarse-grained models of polymers: status and perspectives. *Adv Polym Sci* 152:41–156
81. Honeycutt JD (1998) A general simulation method for computing conformational properties of single polymer chains. *Comput Theor Polym Sci* 8(1–2):1–8. doi:[10.1016/s1089-3156\(97\)00025-1](https://doi.org/10.1016/s1089-3156(97)00025-1)
82. Ahlrichs P, Dunweg B (1999) Simulation of a single polymer chain in solution by combining lattice Boltzmann and molecular dynamics. *J Chem Phys* 111(17):8225–8239. doi:[10.1063/1.480156](https://doi.org/10.1063/1.480156)

83. Havrankova J, Limpouchova Z, Prochazka K (2003) Monte Carlo study of heteroarm star copolymers in good and selective solvents. *Macromol Theory Simul* 12(7):512–523. doi:[10.1002/mats.200350012](https://doi.org/10.1002/mats.200350012)
84. Viduna D, Limpouchova Z, Prochazka K (2001) Monte Carlo simulation of polymer brushes in narrow pores. *J Chem Phys* 115(15):7309–7318. doi:[10.1063/1.1405444](https://doi.org/10.1063/1.1405444)
85. Zhou Z, Daivis PJ (2009) Molecular dynamics study of polymer conformation as a function of concentration and solvent quality. *J Chem Phys* 130(22), 224904. doi:[10.1063/1.3149858](https://doi.org/10.1063/1.3149858)
86. Jusufi A, Likos CN (2009) Colloquium: star-branched polyelectrolytes: the physics of their conformations and interactions. *Rev Mod Phys* 81(4):1753–1772. doi:[10.1103/RevModPhys.81.1753](https://doi.org/10.1103/RevModPhys.81.1753)
87. Jusufi A, Likos CN, Lowen H (2002) Counterion-induced entropic interactions in solutions of strongly stretched, osmotic polyelectrolyte stars. *J Chem Phys* 116(24):11011–11027. doi:[10.1063/1.1480007](https://doi.org/10.1063/1.1480007)
88. Polson JM, Opps SB, Abou Risk N (2009) Theoretical study of solvent effects on the coil-globule transition. *J Chem Phys* 130(24), 244902. doi:[10.1063/1.3153350](https://doi.org/10.1063/1.3153350)
89. Rissanou AN, Anastasiadis SH, Bitsanis IA (2009) A Monte Carlo study of the coil-to-globule transition of model polymer chains near an attractive surface. *J Polym Sci Part B Polym Phys* 47(24):2462–2476. doi:[10.1002/polb.21869](https://doi.org/10.1002/polb.21869)
90. Limbach HJ, Holm C, Kremer K (2004) Conformations and solution structure of polyelectrolytes in poor solvent. *Macromol Symp* 211:43–53. doi:[10.1002/masy.200450703](https://doi.org/10.1002/masy.200450703)
91. Ulrich S, Laguerre A, Stoll S (2004) Complex formation between a nanoparticle and a weak polyelectrolyte chain: Monte Carlo simulations. *J Nanoparticle Res* 6(6):595–603. doi:[10.1007/s11051-004-3548-4](https://doi.org/10.1007/s11051-004-3548-4)
92. Nair AKN, Uyaver S, Sun SY (2014) Conformational transitions of a weak polyampholyte. *J Chem Phys* 141(13):11. doi:[10.1063/1.4897161](https://doi.org/10.1063/1.4897161)
93. Kosovan P, Limpouchova Z, Prochazka K (2008) Charge distribution and conformations of weak polyelectrolyte chains in poor solvents. *Collect Czechoslov Chem Commun* 73(4):439–458. doi:[10.1135/cccc20080439](https://doi.org/10.1135/cccc20080439)
94. Allen MP, Tildesley DJ (1987) *Computer simulation of liquids*. Clarendon, Oxford
95. Odijk T (1977) Polyelectrolytes near the rod limit. *J Polym Sci Part B Polym Phys* 15(3):477–483. doi:[10.1002/pol.1977.180150307](https://doi.org/10.1002/pol.1977.180150307)
96. Skolnick J, Fixman M (1977) Electrostatic persistence length of a wormlike polyelectrolyte. *Macromolecules* 10(5):944–948. doi:[10.1021/ma60059a011](https://doi.org/10.1021/ma60059a011)
97. Khokhlov AR, Khachaturian KA (1982) On the theory of weakly charged poly-electrolytes. *Polymer* 23(12):1742–1750. doi:[10.1016/0032-3861\(82\)90116-1](https://doi.org/10.1016/0032-3861(82)90116-1)
98. Everaers R, Milchev A, Yamakov V (2002) The electrostatic persistence length of polymers beyond the OSF limit. *Eur Phys J E* 8(1):3–14. doi:[10.1140/epje/i2002-10007-3](https://doi.org/10.1140/epje/i2002-10007-3)
99. Nguyen TT, Shklovskii BI (2002) Persistence length of a polyelectrolyte in salty water: Monte Carlo study. *Phys Rev E* 66(2), 021801. doi:[10.1103/PhysRevE.66.021801](https://doi.org/10.1103/PhysRevE.66.021801)
100. Ullner M (2003) Comments on the scaling behavior of flexible polyelectrolytes within the Debye-Huckel approximation. *J Phys Chem B* 107(32):8097–8110. doi:[10.1021/jp027381i](https://doi.org/10.1021/jp027381i)
101. Barrat JL, Joanny JF (1993) Persistence length of polyelectrolyte chains. *Europhys Lett* 24(5):333–338. doi:[10.1209/0295-5075/24/5/003](https://doi.org/10.1209/0295-5075/24/5/003)
102. Micka U, Kremer K (1997) Persistence length of weakly charged polyelectrolytes with variable intrinsic stiffness. *Europhys Lett* 38(4):279–284. doi:[10.1209/epl/i1997-00238-x](https://doi.org/10.1209/epl/i1997-00238-x)
103. Gubarev A, Carrillo J-MY, Dobrynin AV (2009) Scale-dependent electrostatic stiffening in biopolymers. *Macromolecules* 42(15):5851–5860. doi:[10.1021/ma9008143](https://doi.org/10.1021/ma9008143)
104. Manghi M, Netz RR (2004) Variational theory for a single polyelectrolyte chain revisited. *Eur Phys J E* 14(1):67–77. doi:[10.1140/epje/i2004-10007-3](https://doi.org/10.1140/epje/i2004-10007-3)
105. Bacova P, Kosovan P, Uhlik F, Kuldova J, Limpouchova Z, Prochazka K (2012) Double-exponential decay of orientational correlations in semiflexible polyelectrolytes. *Eur Phys J E* 35(6):53. doi:[10.1140/epje/i2012-12053-6](https://doi.org/10.1140/epje/i2012-12053-6)